ORIGINAL ARTICLES
(CC BY-SA)
UDC: 616.36-006-08
DOI: https://doi.org/10.2298/VSP260209029S

Cone-beam computed tomography–guided precise chemoembolization for hypovascular hepatocellular carcinoma

Precizna hemoembolizacija hipovaskularnog hepatocelularnog karcinoma vođena kompjuterizovanom tomografijom konusnog zraka

Chengzi Jun Sun, Jiahui Zhou

Tongxiang First People's Hospital, Department of Gastroenterology, Tongxiang, Zhejiang, China

Abstract

Background/Aim. Hypovascular hepatocellular carcinoma (HCC) remains a therapeutic challenge owing to its inadequate arterial supply and limited responsiveness to standard transarterial chemoembolization (TACE). The aim of this study was to assess the clinical efficacy and safety of cone-beam computed tomography (CBCT) three-dimensional (3D) imaging-guided precise TACE vs. conventional digital subtraction angiography (DSA)-guided TACE in the treatment of hypovascular HCC. **Methods.** A retrospective study was performed on patients with hypovascular HCC who underwent TACE at our institution from January 2020 to December 2023. Using propensity score matching (PSM) with a 1 : 1 ratio, 58 patients were allocated to each of the two groups: the CBCT-guided precise TACE group (CBCT group) and the conventional DSA-guided TACE group (DSA group). Matching covariates included age, gender, Child-Pugh grade, tumor size, and tumor number. Short-term efficacy, long-term survival, and safety profiles were compared between the two groups. **Results.** Three months after the procedure, the CBCT group exhibited a markedly higher objective response rate (63.79% vs. 36.21%) and disease control rate (86.21% vs. 68.97%) compared to the DSA group ($p < 0.05$). Regarding long-term survival, the CBCT group exhibited significantly prolonged median progression-free survival (10.80 months vs. 7.10 months) and a higher 1-year progression-free survival rate (65.52% vs. 41.38%) compared to the DSA group ($p < 0.05$). However, no statistically significant differences were observed between the CBCT and DSA groups for median overall survival (22.50 months vs. 19.10 months) or the 1-year overall survival rate (81.03% vs. 72.41%) ($p > 0.05$). The incidence of post-embolization syndrome and severe complications (e.g., liver abscess, hepatic failure) did not differ significantly across the groups ($p > 0.05$). Notably, the elevation in alanine aminotransferase levels on the third postoperative day was considerably lower in the CBCT group than in the DSA group ($p = 0.016$). **Conclusion.** CBCT 3D imaging-guided precise TACE significantly enhances short-term therapeutic efficacy, prolongs progression-free survival, and provides superior hepatoprotection without increasing procedural risks, establishing it as a safe and effective interventional treatment option for hypovascular HCC.

Keywords:
angiography, digital subtraction; carcinoma, hepatocellular; chemoembolization, therapeutic; cone-beam computed tomography; imaging, three-dimensional; treatment outcome.

Apstrakt

Uvod/Cij. Hipovaskularni hepatocelularni karcinom (*hepatocellular carcinoma* – HCC) i dalje predstavlja terapijski izazov zbog nedovoljne arterijske vaskularizacije i slabog odgovora na standardnu transarterijsku hemoembolizaciju (*transarterial chemoembolization* – TACE). Cilj rada bio je da se procene klinička efikasnost i bezbednost precizne TACE vođene trodimenzionalnim (3D) snimanjem pomoću kompjuterizovane tomografije konusnog zraka (*cone-beam computed tomography* – CBCT) u odnosu na konvencionalnu TACE vođenu digitalnom subtrakcionom angiografijom (DSA) u lečenju hipovaskularnog HCC. **Metode.** Retrospektivnom studijom obuhvaćeni su oboleli od hipovaskularnog HCC koji su bili podvrgnuti TACE proceduri u našoj ustanovi u periodu od januara 2020. do decembra 2023. godine. Korišćenjem metode uparivanja na osnovu skora sklonosti (*propensity score matching* – PSM) u odnosu 1 : 1, po 58 bolesnika raspoređena su u svaku od dve grupe: grupu precizne TACE vođene CBCT (grupa CBCT) i grupu konvencionalne TACE vođene DSA (grupa DSA). Kovarijate podudarnosti obuhvatile su životno doba, pol, Child-Pugh stepen, veličinu i broj tumora. Upoređeni su kratkoročna efikasnost, dugoročno

Correspondence to: Chengzi Jun Sun, Tongxiang First People's Hospital, Department of Gastroenterology, Tongxiang, Zhejiang, 314 500, China. E-mail: chengzijunsun@gmail.com

preživljavanje i bezbednosni profil između ove dve grupe. **Rezultati.** Tri meseca nakon procedure, u grupi CBCT zabeležene su znatno viša stopa objektivnog odgovora (63,79% vs. 36,21%) i stopa kontrole bolesti (86,21% vs. 68,97%) u poređenju sa grupom DSA ($p < 0,05$). U pogledu dugoročnog preživljavanja, grupa CBCT imala je značajno dužu medijanu preživljavanja bez progresije bolesti (10,80 meseci vs. 7,10 meseci) kao i višu jednogodišnju stopu preživljavanja bez progresije bolesti (65,52% vs. 41,38%) u poređenju sa grupom DSA ($p < 0,05$). Međutim, nisu primećene statistički značajne razlike između grupa CBCT i DSA za medijanu ukupnog preživljavanja (22,50 meseci vs. 19,10 meseci), niti za jednogodišnju stopu ukupnog preživljavanja (81,03% vs. 72,41%) ($p > 0,05$). Učestalost postembolizacijskog sindroma i teških komplikacija (npr. apsces jetre, insuficijencija jetre) nije se značajno razlikovala između grupa ($p > 0,05$). Primećeno je da je porast nivoa alanin aminotransferaze trećeg dana posle operacije bio znatno niži u grupi CBCT nego u grupi DSA ($p = 0,016$). **Zaključak.** Precizna TACE vođena 3D CBCT snimanjem značajno poboljšava kratkoročnu terapijsku efikasnost, produžava preživljavanje bez progresije bolesti i obezbeđuje bolju zaštitu jetre bez povećanja rizika od procedure, čime se potvrđuje kao bezbedan i efikasan interventni terapijski izbor za lečenje hipovaskularnog HCC.

Ključne reči:
angiografija, digitalna suptrakcija; karcinom, hepatocelularni; hemoembolizacija, terapijska; kompjuterizovana tomografija konusnog zraka; snimanje, trodimenzionalno; lečenje, ishod.

Introduction

Primary liver cancer (LC) is among the most prevalent malignant neoplasms globally, with consistently elevated morbidity and mortality rates [1]. Transarterial chemoembolization (TACE) is a critical palliative treatment option for most patients with intermediate and advanced stages of LC, forming the foundation of non-surgical therapeutic strategies [2]. However, LC exhibits profound heterogeneity in both biological behavior and imaging manifestations, among which hypovascular hepatocellular carcinoma (HCC) presents a major clinical challenge in treatment. Characterized by the absence of typical tumor staining and abundant neovascularization on conventional digital subtraction angiography (DSA), such tumors often demonstrate arterial-phase enhancement equivalent to or lower than that of the surrounding hepatic parenchyma [3]. The inherent limitations of two-dimensional (2D) DSA imaging hinder clinicians from accurately delineating the true tumor boundaries, infiltration range, and tiny tumor-feeding arteries [4]. Consequently, conventional TACE procedures entail considerable blindness, which is prone to incomplete tumor embolization, residual lesions, and early postoperative recurrence [5]. Meanwhile, the risk of liver function impairment is heightened due to the potential embolization of normal hepatic tissues by embolic agents [6]. In recent years, cone-beam computed tomography (CT) – CBCT technology has emerged as a novel approach to address this predicament [7]. As a three-dimensional (3D) imaging modality integrated into the DSA platform, CBCT enables the rapid acquisition of thin-slice, high soft-tissue resolution 3D images analogous to those obtained *via* multi-detector CT (MDCT) during interventional procedures [8]. A clinical study has demonstrated that CBCT imaging yields a significantly higher detection rate for hepatic tumors–particularly for small and hypovascular lesions–compared with conventional DSA [9]. By fusing CBCT images with preoperative CT or magnetic resonance imaging (MRI) data, clinicians can accurately delineate tumor target volumes in 3D space and clearly identify tumor-feeding vessels that are undetectable on conventional DSA, thereby guiding microcatheter-based superselective catheterization and embolization [10]. Theoretically, this “precision TACE” paradigm can optimize embolization efficacy, improve treatment outcomes, and maximize the preservation of liver function [11]. Nevertheless, systematic clinical research investigating the long-term survival benefits and safety profile of CBCT-guided 3D precision TACE in patients with hypovascular HCC remains insufficient [12].

Based on these considerations, the aim of this study was to conduct a propensity score-matched analysis comparing the short-term efficacy, long-term survival, and safety of CBCT-guided precise TACE vs. conventional DSA-guided TACE in the treatment of hypovascular HCC. This study sought to provide higher-level evidence-based medical support for optimizing clinical interventional therapeutic strategies for this carcinoma subtype.

Methods

The study was approved by the Ethics Committee of the Tongxiang First People’s Hospital, Tongxiang, Zhejiang, China (No. 2020/HCC/11/323, from December 20, 2019). Given the retrospective nature of this analysis and the fact that all patients had completed treatment and entered the follow-up phase at the time of protocol approval, the Institutional Review Board granted a waiver of informed consent. The data collection period spanned from January 2020 to December 2023, with patient data from January 2020 to November 2020 included as historical control data. This research performed a retrospective review of clinical data from patients with HCC who obtained TACE at the institution between January 2020 and December 2023, utilizing the hospital’s medical record system.

The sum of 58 patients with hypovascular HCC who received CBCT-guided precision TACE were initially enrolled. To control confounding bias, propensity score matching (PSM) was performed. With age, gender, Child-Pugh classification, tumor size, and tumor number as key covariates, 58 patients were successfully matched from 215 cases of hypovascular HCC who underwent conventional DSA-guided TACE during the same period, employing the nearest neighbor matching technique with a calliper value of 0.02 at a 1 : 1 ratio. After matching, the standardized differences of all baseline data between the two groups were less than 10%, indicating good intergroup balance.

Inclusion and exclusion criteria

The inclusion criteria were outlined as follows: patients aged 18 to 75 years; confirmed diagnosis of primary HCC by clinical or pathological examinations [13]; preoperative contrast-enhanced CT or MRI demonstrating hypovascular lesions, defined as tumor parenchymal enhancement < 50% of that of surrounding normal hepatic parenchyma during the arterial phase, with this characteristic consistently present in > 50% of tumor volume; liver function classified as Child-Pugh grade A or B; and Eastern Cooperative Oncology Group performance status score of 0 or 1, indicating that patients could tolerate interventional surgery.

Exclusion criteria included the following: presence of extensive extrahepatic metastasis; complicated with significant impairment of essential organs, including the heart, kidneys, and brain; hypersensitivity to iodine-containing contrast agents used in the study; previous history of local liver radiotherapy, ablation, or systemic therapy; and severe deficiency in clinical or follow-up data.

Equipment and materials

All interventional procedures were performed on a DSA system equipped with a flat-panel detector (Artis zee III, Siemens Healthineers, Germany) with integrated CBCT capability (5 s rotational acquisition, 200° scan angle, 0.5 mm reconstruction slice thickness). The used microcatheters included Progreat™ (Terumo, Japan) or Carnelian® (Tokai Medical Products, Japan), with 0.014-inch hydrophilic microguidewires.

Chemotherapeutic agents consisted of epirubicin (50 mg/m²) or lobaplatin (50 mg/m²), mixed with Lipiodol® Ultra Fluid (Lipiodol, Guerbet, France) in a 1 : 1 volume ratio. The emulsion was prepared using a three-way stopcock with repeated aspiration for no less than 10 min. Embolic materials included gelatin sponge particles (350 μm–560 μm, Hangzhou Alicon, China) or polyvinyl alcohol microspheres (300 μm–500 μm, Boston Scientific, USA), selected according to tumor vascularity.

Study groups

After PSM, 58 patients were included in each group, with well-balanced baseline characteristics. All enrolled patients underwent TACE. They were categorized into two groups according to the intraoperative guiding approach: the CBCT-guided precision TACE group (CBCT group) and the conventional DSA-guided routine TACE group (DSA group). All procedures in both groups were performed by the same team of experienced interventional physicians with senior professional titles, so as to minimize operator variability.

Patients in the CBCT group received a standardized precision embolization protocol. The steps for implementing that protocol are described in the text that follows. Firstly, routine angiography and target area confirmation were performed. Patients were put in supine position. Following standard disinfecting and draping, femoral artery puncture and catheterization were performed using the Seldinger approach. The catheter was placed superselectively into the common hepatic artery or proper hepatic artery for conventional DSA angiography, so as to preliminarily evaluate hepatic blood supply and tumor characteristics. For lesions identified as hypovascular on DSA, the CBCT scanning protocol was immediately initiated. Secondly, 3D imaging and pathway planning was performed. The C-arm machine rotated 180°–240° around the patient’s hepatic region, and 3D data were acquired and reconstructed synchronously with contrast agent injection. The reconstructed CBCT images were registered and fused–either automatically or manually–with preoperative contrast-enhanced CT or MRI images. This process enabled accurate 3D delineation of the gross tumor volume (GTV) and the clear identification of tiny tumor-feeding arteries that were not readily visualized on conventional DSA. 3D volume rendering and multi-planar reformation were performed on the workstation. Following identification of tumor-feeding arteries, the optimal working projection was transferred to the DSA system to guide real-time microcatheter superselective cannulation. The third step included superselective embolization and endpoint determination. Under the guidance of 3D imaging, microcatheters were used for superselective catheterization of tumor-feeding arteries. Under real-time fluoroscopic monitoring, chemotherapeutic emulsions (e.g., epirubicin or lobaplatin mixed with lipiodol) were slowly and precisely infused, followed by distal embolization with gelatin sponge particles or polyvinyl alcohol microspheres as appropriate. The embolization endpoint was defined as achieving dense and homogeneous Lipiodol® deposition within the tumor area, as confirmed by intraoperative and postoperative CBCT. The fourth and final step was immediate efficacy verification. Immediately after embolization, a repeat CBCT scan was performed to directly assess the distribution range and homogeneity of Lipiodol® deposition in the tumor from a 3D perspective, so as to verify the completeness of embolization. The detailed procedural workflow of CBCT-guided precise TACE is illustrated in Figure 1.

Patients in the DSA group were treated with 2D DSA imaging guidance alone. Based on the vascular morphology displayed by DSA angiography and personal clinical experience, the operator performed superselective or selective catheterization of suspected tumor-feeding arteries, followed by chemotherapeutic agent infusion and embolization. No CBCT was used for 3D imaging guidance, pathway planning, or immediate postoperative evaluation throughout the procedure in this group.

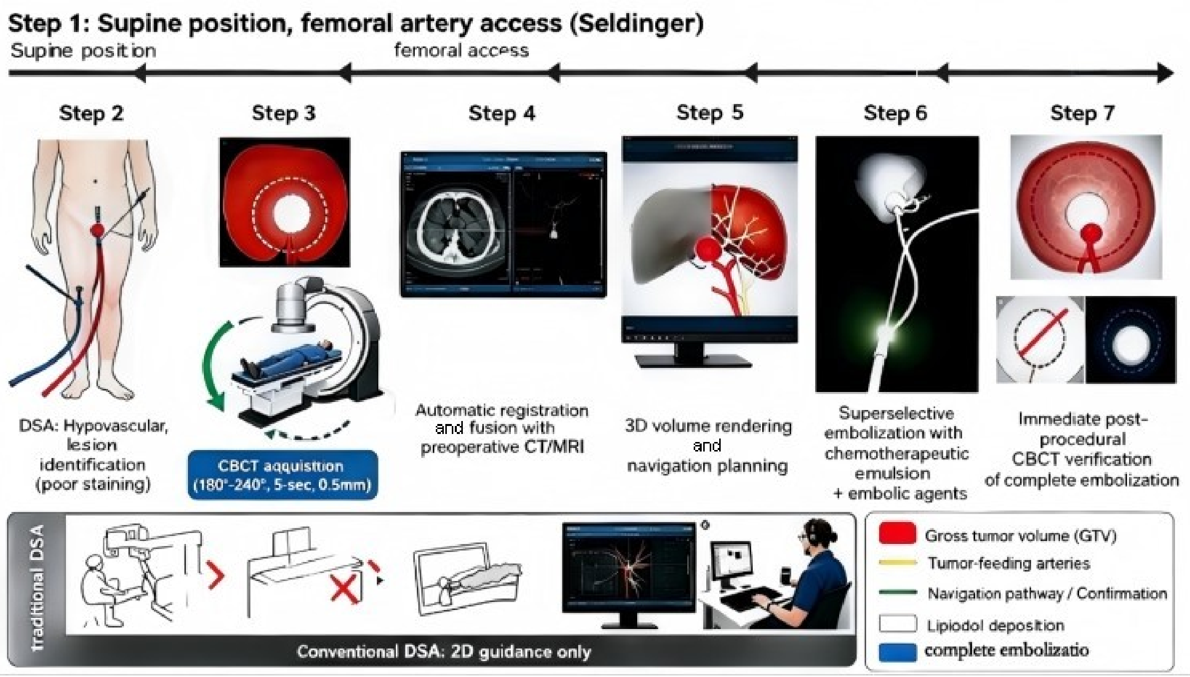

Fig. 1 – Schematic flowchart of cone-beam computed tomography (CBCT)-guided precise transarterial chemoembolization for hypovascular hepatocellular carcinoma.
DSA – digital subtraction angiography; CT – computed tomography; MRI – magnetic resonance imaging; 3D – three-dimensional; 2D – two-dimensional.

TACE treatment in this study was administered on a demand basis. The total intervention cycle was terminated when satisfactory tumor control was achieved, disease progression occurred, or intolerable toxic side effects emerged. All patients underwent regular follow-up after the initial surgery.

Outcome measures

Outcome measures evaluated in this study included short-term efficacy, long-term survival indicators, and safety indicators.

Regarding short-term efficacy, the modified Response Evaluation Criteria in Solid Tumors (mRECIST) were used to assess the outcomes of contrast-enhanced CT or MRI re-examinations 3 months postoperatively. Specifically, the objective response rate (ORR), defined as the percentage of patients attaining complete response (CR) and partial response (PR), and the disease control rate (DCR), defined as the percentage of patients reaching CR, PR, and stable disease, were calculated. CR was defined as complete Lipiodol® deposition throughout the tumor region on post-procedural CT with no residual enhancement on contrast-enhanced imaging at 3 months.

For long-term survival indicators, the study included progression-free survival (PFS) and overall survival (OS). PFS was defined as the time interval from the date of the first TACE treatment to the documentation of radiologically confirmed disease progression or mortality from any cause. Similarly, OS was defined as the duration from the first TACE therapy to mortality from any cause.

Finally, safety indicators focused on the incidence of postoperative complications, including the occurrence rate and severity of post-embolization syndrome (such as fever, pain, nausea, and vomiting) during the acute phase (within 1 week after surgery). Additionally, the dynamic changes in laboratory parameters–namely alanine aminotransferase (ALT), aspartate aminotransferase (AST), and total bilirubin (TBil)–were assessed before surgery, as well as 1, 3, and 7 days postoperatively to evaluate the extent of liver function impairment.

Statistical analysis

All statistical assessments were carried out utilizing SPSS version 26.0. Normally distributed continuous parameters are expressed as mean ± standard deviation and assessed utilizing the independent samples *t*-test. Categorical parameters were expressed as percentages and evaluated *via* the Chi-square test or Fisher's exact test, as applicable. Survival curves are generated utilizing the Kaplan-Meier technique and assessed utilizing the log-rank test for comparison. A two-tailed *p*-value < 0.05 was deemed statistically significant.

Given the retrospective nature of this study, complete raw data for some laboratory parameters could not be extracted from electronic medical records.

Results

No statistically significant differences were observed between the two groups regarding age, sex, Child-Pugh class, tumor size, or tumor number ($p > 0.05$) (Table 1). A mean tumor diameter of 5.4 cm with hypovascular manifestation was observed in this study.

Treatment and follow-up

Patients received a mean of 2.4 ± 0.8 TACE sessions, with a median inter-treatment interval of 5.3 weeks (range: 4–6 weeks). All patients underwent regular follow-up following the initial procedure.

Given the retrospective study design without prospective documentation of “technical success”, we utilized the proportion of cases with clearly evaluable Lipiodol® deposition on immediate post-procedural imaging as a surrogate metric. The resulting image-evaluable rate was 94.83% (55/58) in the CBCT group vs. 72.41% (42/58) in the DSA group, with a statistically significant difference ($p < 0.001$).

Subsequent treatments were evaluated based on available records from our institutional electronic medical record system. During follow-up, approximately 35% of patients in the CBCT group and 40% in the DSA group received subsequent systemic therapy (targeted agents, immunotherapy), while approximately 52% and 59%, respectively, received second-line interventional therapy (radiofrequency ablation, repeat TACE). No significant differences in subsequent treatment patterns were observed between groups. Due to the retrospective nature of this study, some subsequent treatment information was obtained from external institutions, and records were incomplete; therefore, precise case numbers could not be determined.

Comparison of short-term efficacy

The short-term efficacy evaluated using the mRECIST at 3 months after surgery is presented in Table 2. ORR of the CBCT-guided precision TACE group was 63.79% (37/58), greatly surpassing that of the conventional DSA-guided TACE group, 36.21% (21/58), with a statistically significant difference ($p = 0.003$). Regarding the DCR, the CBCT-guided group also exhibited a superior performance (86.21% vs. 68.97%), and the intergroup difference was statistically significant ($p = 0.024$).

Comparison of long-term survival outcomes

A comparison of long-term survival outcomes between the two groups is detailed in Table 3. Survival analysis demonstrated that the median PFS in the CBCT precision TACE group was 10.80 months, which was significantly longer than the 7.10 months observed in the conventional DSA-guided group ($p = 0.013$). In addition, the 1-year PFS rate of the CBCT group (65.52%) was significantly higher than that of the DSA group (41.38%), with a statistically significant difference ($p = 0.024$).

Table 1

Comparison of patients’ baseline data according to groups

Group	Age, years	Male, cases	Child-Pugh class A, cases	Maximum tumor diameter, cm	Number of tumors
CBCT (n = 58)	59.12 ± 8.95	40 (68.97)	48 (82.76)	5.35 ± 1.77	1.45 ± 0.62
DSA (n = 58)	58.78 ± 9.41	42 (72.41)	47 (81.03)	5.41 ± 1.82	1.52 ± 0.71
t/χ^2	0.985	0.172	0.000	0.178	0.563
p-value	0.326	0.678	1.000	0.859	0.575

CBCT – cone-beam computed tomography; DSA – digital subtraction angiography; n – number of patients.
All values are given as numbers (percentages) or mean ± standard deviations.

Table 2

Comparison of the efficacy of different TACE modalities between the two groups at 3 months postoperatively

Group	Complete response	Partial response	Stable disease	Progressive disease	Objective response rate	Disease control rate
CBCT (n = 58)	12 (20.69)	25 (43.10)	13 (22.41)	8 (13.79)	37/58 (63.79)	50/58 (86.21)
DSA (n = 58)	5 (8.62)	16 (27.59)	19 (32.76)	18 (31.03)	21/58 (36.21)	40/58 (68.97)
χ^2					9.103	5.126
p-value					0.003	0.024

TACE – transarterial chemoembolization; CBCT – cone-beam computed tomography; DSA – digital subtraction angiography; n – number of patients.
All values are given as numbers (percentages).

Table 3

Comparison of long-term survival outcomes between the two groups

Group	Median progression-free survival, months	1-year progression-free survival rate, %	Median overall survival, months	1-year overall survival rate, %
CBCT (n = 58)	10.80	65.52	22.50	81.03
DSA (n = 58)	7.10	41.38	19.10	72.41
χ^2	2.478	5.124	1.523	1.256
p-value	0.013	0.024	0.128	0.262

CBCT – cone-beam computed tomography; DSA – digital subtraction angiography; n – number of patients.

Figure 2 illustrates an overview of the OS curves among the groups. With respect to OS, although both the median OS and 1-year overall survival rate of the CBCT group exceeded those of the DSA group (median OS: 22.50 months vs. 19.10 months; 1-year OS rate: 81.03% vs. 72.41%), neither of these differences reached statistical significance ($p > 0.05$) (Figure 2).

Safety comparison

Table 4 illustrates an assessment of safety indicators among the two treatment groups. A lack of statistical significance was observed in the incidence of post-embolization syndrome of any grade (e.g., fever, pain, nausea) between the two groups ($p = 0.784$). Concerning serious complications, no statistically significant differences were observed between the CBCT-guided group and DSA group regarding the incidence of liver abscess (3.45% vs. 5.17%), liver failure (1.72% vs. 3.45%), biliary tract injury (1.72% vs. 3.45%), and nontarget embolization (1.72% vs. 1.72%), with all *p*-values exceeding 0.05. Nevertheless, in terms of biochemical indicators for liver function injury, the amplitude of ALT elevation in the CBCT group on the third day after surgery was significantly lower than that in the DSA group ($p = 0.016$). This finding suggests that precise embolization under CBCT guidance results in less damage to normal liver function.

Discussion

The core challenge of TACE in treating hypovascular HCC lies in achieving sufficient and precise distribution of chemoembolic agents within the tumor parenchyma against the background of atypical blood supply characteristics, while minimizing damage to the surrounding liver function [14, 15]. Although the 3D visualization advantage of CBCT theoretically provides a solution to this dilemma, its comprehensive impact on short-term efficacy, long-term survival, and safety in real-world clinical practice still needs to be verified through rigorous clinical research [16]. By conducting a retrospective cohort analysis, this study systematically compared the clinical efficacy of CBCT-guided precision TACE and the conventional DSA-guided TACE in the management of hypovascular HCC. The results demonstrated that the CBCT-guided group exhibited significantly superior short-term efficacy and long-term PFS,

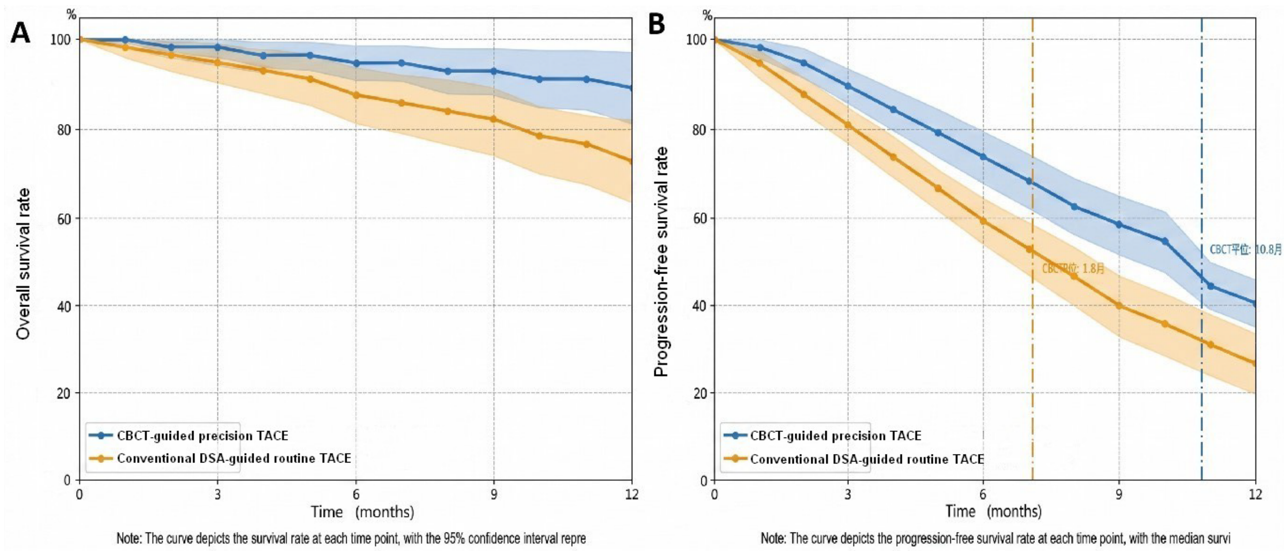

Fig. 2 – Kaplan-Meier curves for overall survival (A) and progression-free survival (B) during one year comparing cone-beam computed tomography (CBCT)-guided and digital subtraction angiography (DSA)-guided transarterial chemoembolisation (TACE).

Table 4

Comparison of postoperative safety profiles between CBCT-guided and conventional DSA-guided TACE groups

Group	Post-embolization syndrome	Liver abscess	Liver failure	Biliary injury	Nontarget embolization	ALT, U/L
CBCT (n = 58)	46/58 (79.31)	2 (3.45)	1 (1.72)	1 (1.72)	1 (1.72)	128.45 ± 70.13
DSA (n = 58)	47/58 (81.03)	3 (5.17)	2 (3.45)	2 (3.45)	1 (1.72)	162.89 ± 79.65
Test statistic	$\chi^2 = 0.075$	Fisher	Fisher	Fisher	Fisher	$t = 2.457$
p-value	0.784	1.000	0.500	1.000	1.000	**0.016**

CBCT – cone-beam computed tomography; DSA – digital subtraction angiography; TACE – transarterial chemoembolization; ALT – alanine aminotransferase; n – number of patients.
All values are given as numbers (percentages) or mean ± standard deviations.
***Note*: Post-embolization syndrome includes fever, pain, nausea/vomiting of any grade within 1 week after the procedure. Severe complications include liver abscess, hepatic failure, biliary tract injury, and nontarget embolization. Values of *p* are derived from the Chi-square test, Fisher's exact test (for categorical variables with expected frequency < 5), or independent samples *t*-test (for ALT). Bold value indicates statistical significance ($p < 0.05$).**

along with notable advantages in liver function preservation. These outcomes are closely associated with the distinct imaging principles and operational precision inherent to the two techniques [17, 18].

In this study, the CBCT-guided group attained markedly superior ORR and DCR at 3 months postoperatively compared with the DSA-guided group. This disparity primarily stems from the fundamental differences between the two imaging modalities [19, 20]. DSA provides 2D vascular images that are plagued by structural overlapping [21]. For hypovascular lesions lacking typical tumor staining characteristics, diagnostic sensitivity is limited, which is prone to missed detection of micro-lesions or misjudgment of the true tumor boundaries [22]. In contrast, CBCT acquires 3D volumetric data through rotational scanning of the C-arm, and the reconstructed tomographic images possess excellent soft tissue resolution, enabling clear visualization of the density differences between the tumor and the surrounding hepatic parenchyma [23]. More importantly, through image fusion and registration with preoperative contrast-enhanced CT or MRI scans, CBCT allows for accurate delineation of GTV in 3D space and identification of micro-tumor-feeding arteries that are otherwise undetectable by conventional DSA [24, 25]. This enhanced "visualization" empowers surgeons to perform true superselective catheterization under guidance, ensuring that chemoembolic agents are more concentrated in the tumor parenchyma, thereby significantly improving the degree of tumor necrosis [26, 27]. This mechanism is directly reflected in the remarkable improvement of short-term efficacy indicators [28].

In terms of long-term survival outcomes, the significant prolongation of median PFS in the CBCT-guided group further confirms the sustained benefits conferred by precision embolization [29]. Complete tumor necrosis and thorough interruption of tumor blood supply fundamentally delay the processes of local recurrence and disease progression [30]. It is noteworthy that although the CBCT-guided group exhibited a trend toward better OS and 1-year OS rate compared with the conventional group, the difference lacked statistical relevance. This observation may be ascribed to multiple factors, including the high inherent heterogeneity of HCC itself, the confounding effects of subsequent treatment modalities (e.g., systemic therapy, second-line interventional procedures) on OS, and the relatively inadequate sample size of this study, which may not possess sufficient statistical power to detect subtle differences in OS. Additionally, for HCC patients, liver function reserve and tumor biological behavior are often more decisive factors influencing long-term prognosis, and the advantages of local treatment may be diluted by other factors during long-term follow-up [31].

Regarding the definition of hypovascular HCC employed in this study, our criterion of "tumor parenchymal enhancement < 50% of surrounding normal hepatic parenchyma" was based on preoperative imaging assessment. While such lesions may encompass some heterogeneous tumors (e.g., with areas of fibrosis or necrosis), this precisely reflects the clinical challenges encountered in TACE treatment [32]. The mean tumor diameter of 5.4 cm with hypovascular manifestation observed in this study may be related to extensive intratumoral fibrosis or necrosis; such lesions indeed present greater challenges in interventional therapy, underscoring the value of CBCT guidance.

The significantly lower ALT elevation observed in the CBCT-guided group (128.45 ± 70.13 U/L vs. 162.89 ± 79.65 U/L, p = 0.016) compared with the DSA-guided group provides compelling biochemical evidence for superior hepatoprotection conferred by precise embolization. This finding is mechanistically rooted in the fundamental technical distinctions between the two modalities. In conventional DSA-guided TACE, the inherent limitations of 2D imaging–namely, structural overlap and poor visualization of hypovascular lesions–frequently result in inadvertent embolization of non-target vessels and unintentional deposition of chemoembolic agents in normal hepatic parenchyma. This "anatomical blindness" triggers bystander ischemic injury and chemical hepatitis in healthy liver tissue, manifesting as elevated transaminases and prolonged hepatic dysfunction.

Conversely, CBCT-guided precision TACE operates through a targeted-sparing paradigm. First, pre-procedural 3D mapping enables accurate delineation of the GTV and the identification of tumor-feeding arteries invisible on conventional DSA. Second, real-time navigation directs microcatheter superselective cannulation exclusively to target vessels. Finally, immediate post-procedural verification confirms dense, homogeneous Lipiodol® deposition confined to the tumor, minimizing spillover to the surrounding liver. This "precision-target, precision-treat, precision-verify" workflow ensures that cytotoxic agents and embolic materials are concentrated within the intended therapeutic zone, thereby maximizing tumor necrosis while minimizing collateral damage.

The clinical significance of this hepatoprotective effect extends beyond the immediate postoperative period. For patients with underlying cirrhosis or limited hepatic reserve–the predominant demographic in HCC populations–preservation of functional liver parenchyma is paramount. Lower ALT elevation on day 3 not only indicates reduced acute hepatocellular injury but also predicts faster recovery of liver function, greater tolerance to subsequent treatment cycles, and expanded opportunities for multimodal therapy, including systemic agents, immunotherapy, or repeat locoregional interventions. In this context, CBCT-guided TACE transforms from a mere technical refinement into a strategic therapeutic advantage that optimizes the long-term treatment trajectory for patients with compromised liver function.

Regarding safety profiles, there were no significant differences in the incidence of post-embolization syndrome and serious complications between the two groups, indicating that the CBCT-guided technique itself does not introduce additional surgical risks. However, the ALT levels in the CBCT-guided group on the third postoperative day were much lower than those in the standard DSA group. This is mainly because during conventional TACE procedures, unclear identification of tumor-feeding arteries on 2D imaging may lead to excessive or inadvertent embolization of non-target vessels. This results in the extravasation and retention of chemoembolic agents in normal liver tissue, triggering more extensive chemical and ischemic liver injury. By accurately identifying tumor-feeding vessels, CBCT-guided precision TACE achieves targeted embolization with high precision. This maximizes the concentration of drugs and embolic agents within the target lesions and effectively reduces damage to normal liver tissue in non-target areas, thus manifesting as a smaller magnitude of postoperative liver enzyme elevation [33]. This advantage is particularly crucial for HCC patients with underlying liver cirrhosis, as superior liver function preservation translates to improved treatment tolerance and expanded opportunities for subsequent therapeutic interventions.

Limitations of the study

This study has several inherent limitations. First, because of its retrospective design, intraoperative “technical success” was not prospectively defined and documented. Instead, we utilized the “image-evaluable rate” as a surrogate metric. Consequently, future studies should employ more standardized definitions of technical success. Second, some subsequent treatment information was obtained from external institutions with incomplete records, which may have influenced the accuracy of the OS analysis. Third, this study employed modified mRECIST criteria for efficacy assessment, but the applicability of these criteria for hypovascular HCC remains limited. Future studies should explore functional imaging modalities, such as diffusion-weighted imaging or positron emission tomography-CT, to establish more appropriate efficacy evaluation systems for hypovascular HCC. Finally, this was a single-center study with a relatively limited sample size. Nevertheless, the results demonstrate that CBCT 3D imaging guidance, through enhanced diagnostic precision and targeting of embolization procedures for hypovascular HCC, effectively improves short-term tumor efficacy, prolongs PFS, and better preserves patient hepatic function. Future larger-sample, prospective randomized controlled studies are warranted to further validate these findings and clarify their ultimate value in improving patient OS.

Conclusion

Cone-beam computed tomography-guided three-dimensional-precision transarterial chemoembolization exhibits enhanced short-term tumor response and significantly extends progression-free survival in patients with hypovascular hepatocellular carcinoma compared to traditional digital subtraction angiography-guided transarterial chemoembolization. This approach allows for precise identification of tumor-feeding arteries, promotes superselective embolization, and provides superior hepatoprotection without elevating operative complications. Despite the absence of a statistically significant improvement in overall survival, the positive effectiveness and safety profile underscore cone-beam computed tomography-guided precision transarterial chemoembolization as a potential interventional approach for this difficult tumor subtype. Comprehensive prospective, multicenter investigations are necessary to further substantiate these results and elucidate their long-term survival advantages.

Conflicts of interest

The authors declare no conflict of interest.

R E F E R E N C E S

1. *Gharaibeh KA, Hamadah AM, El-Zoghby ZM, Lieske JC, Larson TS, Leung N.* Cystatin C Predicts Renal Recovery Earlier Than Creatinine Among Patients With Acute Kidney Injury. Kidney Int Rep 2017; 3(2): 337–42. DOI: 10.1016/j.ekir.2017.10.012.
2. *Sacco R, Tapete G, Simonetti N, Sellitri R, Natali V, Melissari S,* et al. Transarterial chemoembolization for the treatment of hepatocellular carcinoma: a review. J Hepatocell Carcinoma 2017; 4: 105–10. DOI: 10.2147/JHC.S103661.
3. *Hu W, Cao G, Ye S, Xu J, Chen J, Shao G.* Quantitative analysis with multiphase contrast-enhanced computed tomography to evaluate residual tumor activity of hepatocellular carcinoma after DEB-TACE. Medicine (Baltimore) 2023; 102(24): e34054. DOI: 10.1097/MD.0000000000034054.
4. *Bortot B, Mangogna A, Di Lorenzo G, Stabile G, Ricci G, Biffi S.* Image-guided cancer surgery: a narrative review on imaging modalities and emerging nanotechnology strategies. J Nanobiotechnology 2023; 21(1): 155. DOI: 10.1186/s12951-023-01926-y.
5. *Guo J, Zhang X, Kong J.* Prediction of bile duct injury after transarterial chemoembolization for hepatocellular carcinoma: Model establishment and verification. Front Oncol 2022; 12: 973045. DOI: 10.3389/fonc.2022.973045.
6. *Zhao J, Zou Z, Zheng Q, Liu C.* Clinical predictors for liver function impairment and post-embolization syndrome following transcatheter arterial chemoembolization in primary hepatic carcinoma patients: a retrospective study. Am J Cancer Res 2025; 15(5): 2259–74. DOI: 10.62347/PJVG6340.
7. *Venkatesh E, Elluru SV.* Cone beam computed tomography: basics and applications in dentistry. J Istanb Univ Fac Dent 2017; 51(3 Suppl 1): S102–21. DOI: 10.17096/jiufd.00289.
8. *Fahrig R, Jaffray DA, Sechopoulos I, Webster Stayman J.* Flat-panel conebeam CT in the clinic: history and current state. J Med Imaging (Bellingham) 2021; 8(5): 052115. DOI: 10.1117/1.JMI.8.5.052115.
9. *Kim DJ, Chul-Nam I, Park SE, Kim DR, Lee JS, Kim BS,* et al. Added Value of Cone-Beam Computed Tomography for Detecting Hepatocellular Carcinomas and Feeding Arteries during Transcatheter Arterial Chemoembolization Focusing on Radiation Exposure. Medicina (Kaunas) 2023; 59(6): 1121. DOI: 10.3390/medicina59061121.
10. *Zhong BY, Jia ZZ, Zhang W, Liu C, Ying SH, Yan ZP,* et al. Application of Cone-beam Computed Tomography in Interventional Therapies for Liver Malignancy: A Consensus Statement by the Chinese College of Interventionalists. J Clin Transl Hepatol 2024; 12(10): 886–91. DOI: 10.14218/JCTH.2024.00213.

11. *Zhong BY, Jin ZC, Chen JJ, Zhu HD, Zhu XL.* Role of Transarterial Chemoembolization in the Treatment of Hepatocellular Carcinoma. J Clin Transl Hepatol 2023; 11(2): 480–9. DOI: 10.14218/JCTH.2022.00293.
12. *Solim LA, Atasoy D, Vogl TJ.* The efficacy of cone-beam computed tomography-guided transcatheter arterial chemoembolization in hepatocellular carcinoma survival: A systematic review. J Clin Imaging Sci 2024; 14: 25. DOI: 10.25259/JCIS_32_2024.
13. *Chen X, Lu Y, Shi X, Han G, Zhang L, Ni C,* et al. Epidemiological and Clinical Characteristics of Five Rare Pathological Subtypes of Hepatocellular Carcinoma. Front Oncol 2022; 12: 864106. DOI: 10.3389/fonc.2022.864106.
14. *Ebeling Barbier C, Heindryckx F, Lennernäs H.* Limitations and Possibilities of Transarterial Chemotherapeutic Treatment of Hepatocellular Carcinoma. Int J Mol Sci 2021; 22(23): 13051. DOI: 10.3390/ijms222313051.
15. *Kotsifa E, Vergadis C, Vailas M, Machairas N, Kykalos S, Damaskos C,* et al. Transarterial Chemoembolization for Hepatocellular Carcinoma: Why, When, How? J Pers Med 2022; 12(3): 436. DOI: 10.3390/jpm12030436.
16. *Hora BS, Varghese AS, Patil P, Anbalagan S, Chandarani S, Shaik N.* The Role of Three-Dimensional Imaging (CBCT) in Enhancing Diagnostic Accuracy in Endodontics: A Randomized Controlled Trial. J Pharm Bioallied Sci 2024; 16(Suppl 1): S871–3. DOI: 10.4103/jpbs.jpbs_1066_23.
17. *Hricak H, Mayerhoefer ME, Herrmann K, Lewis JS, Pomper MG, Hess CP*, et al. Advances and challenges in precision imaging. Lancet Oncol 2025; 26(1): e34–45. DOI: 10.1016/S1470-2045(24)00395-4.
18. *Kantarcı M, Aydın S, Oğul H, Kızılgöz V.* New imaging techniques and trends in radiology. Diagn Interv Radiol 2025; 31(5): 505–17. DOI: 10.4274/dir.2024.242926.
19. *Frush DP, Callahan MJ, Coley BD, Nadel HR, Paul Guillerman R.* Comparison of the different imaging modalities used to image pediatric oncology patients: A COG diagnostic imaging committee/SPR oncology committee white paper. Pediatr Blood Cancer 2023; 70 Suppl 4(Suppl 4): e30298. DOI: 10.1002/pbc.30298.
20. *Waite S, Scott J, Colombo D.* Narrowing the Gap: Imaging Disparities in Radiology. Radiology 2021; 299(1): 27–35. DOI: 10.1148/radiol.2021203742.
21. *Sekiguchi Y, Okamoto T, Matsuzawa T, Fujimoto K, Fujiwara K, Kondo T*, et al. PatchDSA: improving digital subtraction angiography with patch-based phase-matching in natural breathing scenarios. Radiol Phys Technol 2025; 18(3): 698–706. DOI: 10.1007/s12194-025-00922-1.
22. *Tabu K, Mawatari S, Oda K, Kumagai K, Inada Y, Uto H,* et al. Hypovascular tumors developed into hepatocellular carcinoma at a high rate despite the elimination of hepatitis C virus by direct-acting antivirals. PLoS One 2020; 15(8): e0237475. DOI: 10.1371/journal.pone.0237475.
23. *Floridi C, Radaelli A, Abi-Jaoudeh N, Grass M, Lin M, Chiaradia M,* et al. (2014). C-arm cone-beam computed tomography in interventional oncology: technical aspects and clinical applications. Radiol Med 2014; 119(7): 521–32. DOI: 10.1007/s11547-014-0429-5. Erratum in: Radiol Med 2015; 120(4): 406. DOI: 10.1007/s11547-014-0450-8.
24. *Cheung AL, Zhang L, Liu C, Li T, Cheung AH, Leung C,* et al. Evaluation of Multisource Adaptive MRI Fusion for Gross Tumor Volume Delineation of Hepatocellular Carcinoma. Front Oncol 2022; 12: 816678. DOI: 10.3389/fonc.2022.816678.
25. *Song Y, Erickson B, Chen X, Li G, Wu G, Paulson E*, et al. Appropriate magnetic resonance imaging techniques for gross tumor volume delineation in external beam radiation therapy of locally advanced cervical cancer. Oncotarget 2018; 9(11): 10100–9. DOI: 10.18632/oncotarget.24071.
26. *de Baere T, Ronot M, Chung JW, Golfieri R, Kloeckner R, Park JW*, et al. Initiative on Superselective Conventional Transarterial Chemoembolization Results (INSPIRE). Cardiovasc Intervent Radiol 2022; 45(10): 1430–40. DOI: 10.1007/s00270-022-03233-9.
27. *Lu J, Zhao M, Arai Y, Zhong BY, Zhu HD, Qi XL*, et al. Clinical practice of transarterial chemoembolization for hepatocellular carcinoma: consensus statement from an international expert panel of International Society of Multidisciplinary Interventional Oncology (ISMIO). Hepatobiliary Surg Nutr 2021; 10(5): 661–71. DOI: 10.21037/hbsn-21-260.
28. *Samiee R, Jameie M, Rahmati M, Looha MA, Mobader S, Tafakhori A*, et al. Short-term efficacy of peripheral nerve stimulation for essential tremor in a randomized double-blind controlled trial. Sci Rep 2025; 15(1): 28713. DOI: 10.1038/s41598-025-13487-1.
29. *Rostambeigi N, Crawford D, Golzarian J.* Benefits and advances of Cone Beam CT use in prostatic artery embolization: review of the literature and pictorial essay. CVIR Endovasc 2024; 7(1): 46. DOI: 10.1186/s42155-024-00459-1.
30. *Lugano R, Ramachandran M, Dimberg A.* Tumor angiogenesis: causes, consequences, challenges and opportunities. Cell Mol Life Sci 2020; 77(9): 1745–70. DOI: 10.1007/s00018-019-03351-7.
31. *Nishida N.* Long-term prognosis and management of hepatocellular carcinoma after curative treatment. Clin Mol Hepatol 2020; 26(4): 480–3. DOI: 10.3350/cmh.2020.0208.
32. *Lanza C, Ascenti V, Amato GV, Pellegrino G, Triggiani S, Tintori J*, et al. All You Need to Know About TACE: A Comprehensive Review of Indications, Techniques, Efficacy, Limits, and Technical Advancement. J Clin Med 2025; 14(2): 314. DOI: 10.3390/jcm14020314.
33. *Wan YX, Lin ZY, Chen LT, Wu RQ, Zhang Y, Du ZQ.* Arterial and biliary complications after transarterial chemoembolization for hepatocellular carcinoma. World J Clin Oncol 2026; 17(1): 113618. DOI: 10.5306/wjco.v17.i1.113618.

Received on February 9, 2026
Revised on March 16, 2026
Revised on April 18, 2026
Accepted on April 29, 2026
Online First May 2026